FeB/Fe_2B Phase Transformation during SPS Pack-Boriding: Boride Layer Growth Kinetics

L. G. YU [a], X. J. Chen [a], K. A. Khor [a†] and G. Sundararajan [b]

[a] *School of Mechanical and Production Engineering, Nanyang Technological University, Nanyang Avenue, Singapore 639798, Singapore*

[b] *International Advanced Research Centre for Powder Metallurgy and New Materials* (*ARCI*), *Balapur* (*PO*), *R.R. District, Hyderabad 500 005, India*

ABSTRACT

The iron boride layer growth kinetics in mild steel through the spark plasma sintering (SPS) pack-boriding technique is investigated at 850˚C with different boriding durations (maximum 240 minutes). Results show that when the boriding duration is shorter than 90 minutes, both FeB and Fe_2B layers would form and grow on the mild steel surface with the FeB layer on the top of Fe_2B sub-layer. However, with further increase in boriding duration, the top FeB layer eventually ceases growing, starts to diminish, and, finally disappears completely by transforming into the Fe_2B phase. Numerical simulation is implemented to explain this phenomenon. Subsequently, the diffusion coefficient of boron in FeB and Fe_2B phase is obtained through fitting the experimental results into the model. The simulation results are found to be in good agreement with the experimental results, and the estimated diffusion coefficients of boron in FeB and Fe_2B phases as 2.33×10^{-9} and 4.67×10^{-9} cm^2/s, respectively. Both the simulation and experimental results reveal that the Fe_2B monophase layer can be obtained through the transformation of FeB to Fe_2B phase due to the depletion of boron concentration in the boriding medium, and is indifferent to the formation of FeB phase at the very onset of the boriding process. This provides a new approach to overcome the side effect of FeB formation in borided components.

Keywords: *Boriding, phase transformation, FeB, Fe_2B, boron depletion, layer growth kinetics*

† Corresponding author: fax: 65 6 791 1859 email: mkakhor@ntu.edu.sg

1. INTRODUCTION

Boriding (or Boronizing) is an important thermo-chemical treatment applied to enhance the surface hardness and wear resistance of ferrous and non-ferrous alloy components [1, 2]. In the boriding process, boron atoms diffuse into the surface of a workpiece and form borides with the base metal. Boriding can be carried out in solid, liquid or gaseous media [3]. Among the various boriding processes, solid-state pack boriding is the most frequently used. And industrial boriding is predominantly applied to steel and ferrous alloys. Yet the pack-boriding process has the disadvantages of requiring relatively high processing temperature (800-1000˚C) and long process duration (~3-16h) to obtain an effective boride layer thickness [4, 5]. So in the past 20 years, studies have been carried out to decrease the boriding temperature and/or the boriding duration. It has been shown that ion implantation boriding [3, 6] and plasma-assisted boriding [4-8] can effectively decrease the boriding temperature. And the application of spark plasma sintering (SPS) technique in boriding effectively lowers the boriding temperature, and shortens the boriding duration at the same time, due to the activation of the pack boriding medium as well as the workpiece with a high current discharge [9].

The formation of iron borides (FeB and Fe_2B) occurred through the diffusion of B into mild steel. The thickness of the boride layer is determined through the processing temperature and duration of the treatment, as well as, the chemical composition of the steel [10], and the boron potential in the pack mixture [11]. The boride layer growth kinetics has been extensively studied [11-23]. Generally, for the practical applications, the formation of a mono-phase (Fe_2B) with saw-tooth morphology is more desirable than a dual-phase layer comprising of FeB and Fe_2B [1, 2, 11, 12]. This is because, although the boron rich FeB phase is decidedly harder, it is more brittle than the iron sub-boride, Fe_2B phase. Furthermore, crack formation is often observed at the FeB/Fe_2B interface of a dual-phase layer, as FeB and Fe_2B phases exhibit substantially different coefficients of thermal expansion. These cracks often lead to flaking and spalling when a mechanical load is applied. By controlling the boronizing process parameters, especially by limiting the boron potential of the boriding media [11, 12], Fe_2B phase can be consistently achieved during pack boriding. Yet, lowering the boron concentration inevitably slows down the boron diffusion process. In return, longer boriding duration is necessary for a desired boride layer thickness.

In reality, the side effect of FeB phase can be mitigated. As FeB phase can transform into Fe_2B phase through heat treatment at high temperature [22], and the boriding processes

are usually carried out at high temperatures, hence through prolonging the boriding duration, one can primarily transform FeB phase into Fe_2B phase. In this treatment, it is essential to ensure that boron in the boriding mixture is depleted so that there is insufficient boron potential for FeB phase formation. As the treatment is carried out in the boriding process, it is economically cheaper compared to carrying out another post-boriding heat-treatment. Also the thermal expansion difference is no longer a problem, as there will be very few FeB phase remaining on the surface of the workpiece when it is cooling down.

Recent study has shown that heat treatment at high temperatures can lead to the FeB → Fe_2B phase transformation [22]. Brakman et al. [23] reported that the decrease of the boron potential in the boriding process may lead to a stop or even a shrinking of the FeB layer growth, although the overall boride-layer increased. But up to now, there is no systematic study on the effect of boron depletion on the boride layer growth kinetics. Also there is no report on obtaining Fe_2B monophase layer from FeB/Fe_2B double phase layer by prolonging the boriding process under a boron depletion condition.

In this paper, mild steel samples are borided by the spark plasma sintering pack-boriding technique (SPS boriding). The effect of boron depletion in the boriding pack mixture on the boriding layer composition and thickness is examined. Scanning electron microscope (SEM) was used to characterize the microstructure of the boriding layer. X-Ray Diffraction (XRD) was used to identify the phase composition of the boriding layer. A theoretical model was employed to describe the phenomenon, taking into account the depletion of the boron-concentration in the boriding pack during the boriding process.

2. EXPERIMENTAL DETAILS

Mild steel of grade AISI 1018, with a carbon content of 0.2%, was used. The mild steel rod with diameter of 13 mm was cut into discs of thickness 5 mm for each disc. The sample disc was ground, polished and cleaned with acetone before being loaded into the graphite die set. The sample w as then packed into a Φ=20 mm die with the boriding powder pack materials having 5 mm buffer on each side of the sample. The boriding powder mixture (boriding media) contains B_4C as the born source, an activator to deposit atomic boron at the workpiece and, SiC as the diluent. The SPS system DR SINTER Model 1050 (Sumitomo Coal Mining (SCM), Japan) was used for the boriding of the mild steel samples. The

boriding process was carried out only at 850°C for different durations of 5, 15, 30, 60, 120 and 240 minutes.

After SPS boriding, the as-borided mild steel discs were cut diameter-wise for characterization. The JEOL JSM-5600LV SEM equipment was used to study the microstructure of the boriding layer. The Philips 7198W XRD equipment was used to identify the different phases contained in the sample. In order to obtain the composition difference between the external layer and the interior layer, grazing XRD is carried out for the samples borided for 30 minutes and 60 minutes. Reitveld refinement is carried out for all XRD results to obtain the depth-weighted phase fractions and the preferred orientation information of the phases in each sample. Due to the fiber texture nature of the boride layers, the March-Dollase parameter, $\boldsymbol{r}$ ($0< \boldsymbol{r} <1$, $\boldsymbol{r} = 1$ stands for no preferred orientation) is used to express the preferred orientation. The preferred orientation results are compared to that of the mild steel substrate.

The measurement of layer thickness is exceedingly crucial for the study of boride layer growth kinetics. Yet, since the borided coating has finger-like projections, the definition of coating thickness is not immediately obvious. Brakman et al. [23] only selects the FeB or Fe_2B needles which penetrating most deeply for indication of layer thickness. The values are obtained as averages over 10 measurements taken along a distance of 5 mm parallel to the surface of the specimen. Jain et al. [11] use the procedure suggested by Chatterjee-Fisher [2], in which the average finger height is used to describe the thickness of the coating. But these two methods do not take the finger width into account. In order to consider the finger height and the finger width together, the present study suggests using the boride layer area (including the area of all fingers), $\boldsymbol{A}$, divided by the boride layer length, $\boldsymbol{l}$, to calculate the boride layer thickness, $\boldsymbol{d}$, as depicted in Equation (1) and Fig. 1:

$$d = \frac{A}{l} \qquad (1)$$

A simple picture-processing procedure is conducted, and a program is developed to calculate the area of the borided layer.

3. EXPERIMENTAL RESULTS AND DISCUSSION

Fig. 2 presents the XRD results of the mild steel samples borided at 850˚C for various durations. From Fig. 2, it is obvious that for mild steel samples with a boriding time of 5, 15 and 30 minutes, a combination of FeB and Fe_2B phases is detected through XRD. As the FeB

top layers formed after 5, 15 and 30 minutes of boriding are still thin, both FeB and Fe_2B phases can be detected simultaneously by XRD. For the mild steel borided for 60 minutes, the FeB top layer is thick enough to mask the Fe_2B sublayer so that only FeB phase is detected by XRD. For the sample that is SPS borided for 90 minutes, the sample surface is dominated by FeB phase, but the (002) peak of Fe_2B is clearly detected. For the 120-minutes sample, Fe_2B dominates the sample surface, and the FeB phase is hardly detected.

In order to obtain the depth-weighted phase composition and the preferred orientation information in the boriding layer of each sample, Rietveld refinement is applied to all XRD patterns, and the results are shown in Table I. The results confirm the above discussion. The preferred orientation results show that both FeB and Fe_2B sublayers exhibit a (002) preferred orientation, and the Fe_2B (002) preferred orientation becomes increasingly sharp for longer boriding duration [23]. Similar behavior is probable for the FeB (002) preferred orientation, but is not observed in the results, because FeB layer is always very thin. Compared to the strongly preferred orientation developed in the boride sublayers, the mild steel substrate shows no preferred orientation, as shown in Table I. One can conclude that the preferred orientation in the boride layer is not related to the mild steel substrate. The finger-like growth is caused by the anisotropic crystallographic nature of the FeB (tetragonal) and Fe_2B (Orthorhombic) phases, and the [001] is the easiest boron diffusion direction for both phases, which is independent of the mild steel substrate.

Fig. 3 shows the grazing XRD results for the samples borided for 30 minutes and 60 minutes. The Rietveld results are also shown in Table I. For a grazing angle of 2 degrees, no diffraction peak can be detected. This is because the roughness of the sample is increased after boriding, and a grazing angle of 2 degrees is not enough to obtain diffraction signal from the sample. At a grazing angle of 5 and 10 degrees, the XRD patterns are dominated by FeB phase for both samples, showing that the external layer is indeed dominated by FeB.

The XRD results indicate that the boriding process is divided into three stages: in the first stage, when the adsorbed boron concentration (the effective boron concentration), $C_{\text{ads}}^{\text{B}}$, on the sample surface is sufficiently high for FeB formation, both FeB and Fe_2B phases are formed and proceed to grow; in the second stage, when the adsorbed boron concentration, $C_{\text{ads}}^{\text{B}}$, on the sample surface is in the range of $C_{\text{up}}^{\text{Fe}_2\text{B}} < C_{\text{ads}}^{\text{B}} < C_{\text{low}}^{\text{FeB}}$ ($C_{\text{up}}^{\text{Fe}_2\text{B}}$ is the upper limit of boron concentration in Fe_2B phase, and $C_{\text{low}}^{\text{FeB}}$ is the lower limit of boron concentration in FeB phase), then the FeB phase will diminish in stead of increasing, but the overall boride

layer is still growing till all the FeB phase is consumed or till $C_{\text{ads}}^{\text{B}} < C_{\text{low}}^{\text{Fe}_2\text{B}}$, depending on which condition fulfills first; in the third stage, the FeB phase is consumed and the condition $C_{\text{ads}}^{\text{B}} < C_{\text{low}}^{\text{Fe}_2\text{B}}$ is attained, and ultimately, the overall boride layer stops growing.

Fig. 4 shows the SEM microstructure of the mild steel samples borided at 850˚C for different durations. The mild steel samples borided at 850˚C for 5 and 30 minutes show a boride film with a thin FeB stratum on top of the Fe_2B layer. As the FeB phase is decidedly more brittle than Fe_2B, and cracks are more easily initiated in FeB phase due to thermal expansion coefficient mismatch between FeB and Fe_2B, the FeB top stratum on the samples borided at 850˚C for 5 minutes is chipped of after polishing and etching. The sample borided for 60 minutes has a continuous FeB phase with thickness over 20 μm. The samples borided for 120 and 240 minutes show almost Fe_2B monolayer. The overall boride layer thicknesses are given in Table II, and depicted in Fig. 5.

4. BORIDE LAYER GROWTH KINETICS

From previous result analysis, the boriding processes may involve six elementary physi-chemical processes as following:

1. $\text{B(free)} \rightarrow \text{B(adsorption)}$
2. $\left.\begin{array}{ll} \text{B(adsorption)} + \text{Fe} \rightarrow \text{FeB} & \text{if } C_{\text{ads}}^{\text{B}} > 0.5 \\ \text{B(adsorption)} + 2\text{Fe} \rightarrow \text{Fe}_2\text{B} & \text{if } 0.33 < C_{\text{ads}}^{\text{B}} < 0.5 \end{array}\right\}$ at B/Fe interface
3. B atoms jump through FeB or Fe_2B lattice from high chemical potential side to low chemical potential side;
4. $\text{Fe}_2\text{B} + \text{B} \rightarrow 2\text{FeB}$ at FeB/Fe_2B interface
5. $2\text{Fe} + \text{B} \rightarrow \text{Fe}_2\text{B}$ at Fe_2B/Fe interface
6. $2\text{FeB} \rightarrow \text{Fe}_2\text{B} + \text{B}$ phase transformation

Among the six elementary boriding steps, one or several steps can be the rate-determining steps for the boride growth. It was reported that at high temperatures, the boride layer growth satisfies parabolic growth, which was attributed to the B diffusion, e.g. step 3, to be the rate-determining step. However, the existing experimental results suggest two

different growth phenomena: (*i*) the FeB sublayer almost disappears after 150 minutes boriding time; (*ii*) the total boriding growth (FeB+Fe_2B) deviates from the parabolic growth after 90 minutes boriding time and stops after 150 minutes boriding time. These two abnormal phenomena were not reported in literature although many studies have been done on the boride layer growth kinetics [11-23]. From the experimental results presented above, one can clearly see that the boron depletion at B/FeB (or B/Fe_2B) interface during boriding process plays an essential role in determining the composition and the thickness of the boride layer.

At the exact onset of the boriding process, when the boron potential is sufficiently high for the formation of FeB phase, this phase will form at the surface of the mild steel. When a continuous FeB thin film is produced, any additional formation of FeB depends on the diffusion of boron through this FeB layer to reach the FeB/Fe interface, resulting in the formation and the growth of Fe_2B phase at the interface of FeB phase and mild steel substrate. As long as the effective boron concentration is greater than the lower limit of boron concentration in FeB, this phase will grow. As the boriding process continues, the boron concentration in the boriding media mixture eventually depletes. At a certain point, it reaches the lower limit of FeB phase, and consequently the growth of FeB phase stops. Yet, the growth of Fe_2B phase continues by consuming the FeB phase. So from this point onwards, even though the overall boride layer thickness continues to increase, the FeB phase layer thickness diminishes. Finally, the Fe_2B phase stops growing when the initial FeB phase is wholly consumed, and the effective boron concentration is lower than the lower limit of Fe_2B phase formation.

In order to simulate the SPS boriding processes, a numerical simulation program is developed. Assuming that (*i*) the interface reactions are sufficiently fast enough so that the boron diffusion is the controlling factor of layer growth; (*ii*) the FeB and Fe_2B phase have the small homogeneity range of 1 at. % and the boron concentration in steel is negligible; (*iii*) the diffusion coefficients are constant within the diffusion layers. In order to simplify the simulation, the volume change during the phase transformation is not considered. Thus, the diffusion system can be separated into three phases: FeB phase, Fe_2B phase and Fe phase. The boron diffusion through the respective phases satisfies the following equations:

$$\frac{\partial C}{\partial t} = D_i \frac{\partial^2 C}{\partial x^2} \qquad (2)$$

(i=1 for 0<x<u and i=2 for u<x<v), where $D_1$and D_2 are the diffusion coefficients within FeB phase and Fe_2B phase. u and v are the location of FeB/Fe_2B and Fe_2B/Fe interfaces, respectively. Since only Fe phase is present before boriding, the initial condition can be written as:

$$C_{Fe_2B} = 0; \quad C_{FeB} = 0 \quad \text{at } x=0 \text{ and } t>0 \tag{3}$$

Fig. 6 illustrates the boron concentration distribution along the depth from the sample surface. Assuming that C_{up}^{FeB} , C_{low}^{FeB} , $C_{up}^{Fe_2B}$ and $C_{low}^{Fe_2B}$ are the upper and lower limit of boron concentration in FeB and Fe_2B phases respectively, the boundary conditions are:

$$\left.\begin{array}{ll} C = C_{up}^{FeB} & \text{for } C_{ads}^{B} > 0.5 \\ C = C_{low}^{FeB} & \text{for } C_{ads}^{B} < 0.5 \text{ and with FeB phase} \\ C = C_{up}^{Fe_2B} & \text{for } 0.33 < C_{ads}^{B} < 0.5 \text{ and without FeB phase} \\ C = C_{low}^{Fe_2B} & \text{for } C_{ads}^{B} < 0.33 \text{ and without FeB phase} \end{array}\right\} \text{ at } x = 0 \tag{4}$$

$$C = C_{low}^{FeB} \qquad \text{at } x=u\text{-}0 \tag{5}$$

$$C = C_{up}^{Fe_2B} \qquad \text{at } x=u\text{+}0 \tag{6}$$

$$C = C_{low}^{Fe_2B} \qquad \text{at } x=v\text{-}0 \tag{7}$$

$$C = 0 \qquad \text{at } x=v\text{+}0 \tag{8}$$

The growth of FeB and Fe_2B layers vs. dt occurs with the simultaneous "consumption" of Fe_2B and Fe at FeB/Fe_2B and Fe_2B/Fe interfaces respectively. Thus, the B should be conserved at the phase interface.

$$(C_{low}^{FeB} - C_{up}^{Fe_2B})du = \left[-D_1 \left(\frac{\partial C}{\partial x} \right)_{u-0} + D_2 \left(\frac{\partial C}{\partial x} \right)_{u+0} \right] dt \tag{9}$$

$$C_{low}^{Fe_2B} dv = \left[-D_2 \left(\frac{\partial C}{\partial x} \right)_{v-0} \right] dt \tag{10}$$

These mass-balance equations can satisfy all values of *t* if the FeB phase exists. Otherwise only Eq. (10) and boundary conditions Eqs. (4, 7 and 8) are needed to solve the diffusion equations.

The effective boron concentration (the adsorbed boron concentration), $c_{\text{ads}}^{\text{B}}$, depletes according to the modified Knudsen evaporation equation:

$$C_{\text{ads}}^{\text{B}} = \frac{f(\theta)P(t)}{\sqrt{2\pi mkT}} \exp(-E_a / RT) \qquad (11)$$

Where E_a is the activation energy for adsorption and $f(\theta)$ is the function of the existing surface coverage of adsorbed species. $P(t)$ is the partial pressure of boron potencial in the boriding media which is changing with time *t*. *m* is mass of one boron atom, *T* is the absolute temperature. *k* and *R* are the Boltzmann Constant and the Gas Constant respectively.

As $K(T) = \frac{f(\theta)}{\sqrt{2\pi mkT}} \exp(-E_a / RT)$ is a constant for fixed temperature, and suppose the emission of boron follows the exponential form: $P(t) = a\ e^{-bt}$, the equation can be rewritten as:

$$C_{ads}^{B} = aK(T)e^{-bt} \qquad (11a)$$

The experimental results of present study show that the FeB phase stops growing after about 90 minutes boriding. And the whole boride layer stops growing after about 120 minutes boriding. By substituting these conditions in equation (11a), the constants $aK(T)$ and *b* in equation (11a) can be determined.

The simulation results are depicted in Fig. 7 together with the experimental results. The simulation results are in reasonable agreement with the experimental results with the estimated diffusion coefficients of boron in FeB and Fe_2B phases of 2.33×10^{-9} and 4.67×10^{-9} cm^2/s, respectively. It is found that the FeB layer reaches maximum thickness after boriding duration of 77 minutes, then gradually reduces and almost completely disappears after boriding duration of 145 minutes. The simulated growth behavior of the FeB layer is confirmed by the XRD results in Fig. 2.

4. CONCLUSION

Mild steel samples are borided by SPS pack-boriding at 850˚C with different treatment durations. The growth of FeB and Fe_2B boride layer on the mild steel surface is investigated using XRD and SEM experiments. Two abnormal phenomena, previously unreported, are discovered in this study: (*i*) the FeB sublayer virtually disappears after 150 minutes of boriding process, and (*ii*) the total boriding growth (FeB+Fe_2B) deviates from the parabolic growth after 90 minutes boriding, and, stops after 150 minutes of pack-boriding. These phenomena can be ascribed to the competition between two concomitant processes: the formation of FeB phase and the phase transformation from FeB phase to Fe_2B phase at the boriding temperature. The competition between the above two processes is controlled by the boron potential in the boriding media. When the boron potential in the boriding media is sufficiently high, the FeB formation process will be dominant and the FeB top layer will proceed. With the extension of boriding process, the boron potential in boriding media depletes. At certain boriding duration, the boron potential becomes inadequate. Consequently, the FeB phase cannot grow further, and after that any additional growth of the boride layer depends only on the consuming of FeB phase. As a consequence, a Fe_2B mono-phase layer can be ultimately obtained when the previously formed FeB phase is completely transformed. A simple model is proposed to describe the above mentioned processes, taking into account the boron concentration depletion in the boriding media during the boriding process. The result of the present paper also gives a new approach to understand the formation of Fe_2B monolayer from FeB/Fe_2B polyphase layer. By prolonging the boriding process, Fe_2B monolayer can be obtained as a result of $FeB \rightarrow Fe_2B$ phase transformation under a boron depletion condition.

REFERENCES

[1] Sinha AK. Boriding (Boronizing). In: Lampman SR, Zorc TB, Daquila JL and Ronke AW, editors. ASM Handbook, Vol. 4. Heat Treating. ASM International, Materials Park (OH), 1991. p.437.

[2] Chatterjee-Fisher R. Boriding and Diffusion Metallizing. In: Sundarshan TS, editor. Surface Modification Technologies, Chapter 8, Marcel Dekker Inc, New York, 1989. p.567.

[3] Davis JA, Wilbur PJ, Williamson DL, Wei R and Vajo JJ. Surf Coat Technol 1998;**103–104:**52

[4] Bartsch K, Leonhardt A. Surf Coat Technol 1999;**116–119**:386

[5] Miyashita F, Yokota K. Surf Coat Technol 1996;**84:**334

[6] Blawert C, Mordike BL and Weisheit A. Surf Coat Technol 1997;**93:**297

[7] Rie KT. Surf Coat Technol 1999;**112:**56

[8] Rodriguez Cabeo E, Laudien G, Biemer S, Rie KT, Hoppe S. Surf Coat Technol 1999;**116–119:**229

[9] Yu LG, Khor KA, and Sundararajan G. Surf Coat Technol 2002;**157**:226

[10] Carbucicchio M and Palombarini G. J Mat Sci Lett 1984;**3:**1046

[11] Jain V and Sundararajan G. Surf Coat Technol 2001;**149:**21

[12] Martini C, Palombarini G, and Carbucicchio M. J Mat Sci 2004;**39:**933

[13] Campos I, Oseguera J, Figueroa U, Garcia JA, Bautista O and Kelemenis G. Mater Sci & Eng A 2003;352:261

[14] Genel K, Ozbek I and Bindal C. Mater Sci & Eng **A** 2003; **347:**311

[15] Pelleg J and Judelewicz M. Thin Solid Films 1992;**215:**35

[16] Genel K, Ozbek I, Kurt A and Bindal C. Surf Coat Technol 2002;**160:**38

[17] Dorofeev VY, Selevtsova IV. Powder Metall & Met Ceram 2001;**40:**19

[18] Chen FS, Wang KL. Surf Coat Technol 1999;**115**:239

[19] Cabeo ER and Rie KT. Material Wissenschaft und Werkstofftechnik 2000;31:345

[20] Nam KS, Lee KH, Lee SR and Kwon SC. Surf Coat Technol 1998;**98:**886

[21] Brandstötter J and Lengauer WJ. J Alloy & Compd 1997;**262:**390

[22] Yan PX, Zhang XM, Xu JW, Wu ZG and Song QM. Mater Chem & Phys 2000;**71:**107

[23] Brakman CM, Gommers AWJ and Mittemeijer EJ. J Mater Res 1989;**4:**1354

Table I. Phase fractions (***f***) and preferred orientation (***r***) calculated by Rietveld refinement (Preferred orientation is calculated by the March-Dollase Model)

Sample			FeB		Fe_2B	
			f	***r***	***f***	***r***
Boriding duration	5 min		0.35	0.57	0.65	0.86
	15 min		0.50	0.39	0.50	0.77
	30 min		0.66	0.53	0.34	0.69
	60 min		0.92	0.61	0.08	0.72
	120 min		0.33	0.74	0.67	0.43
Grazing XRD	30 min	5 deg	0.99	0.74	0.01	0.34
		10 deg	0.97	0.50	0.03	0.41
	60 min	5 deg	0.98	0.66	0.02	0.69
Mild steel substrate			***r*** = 0.98			

Table II. The boride layer thickness for different samples

Boriding duration (minutes)	5	15	30	60	90	120	240
Boride Layer Thickness (μm)	13.6	25.1	34.2	67.8	86.9	97.4	101.9

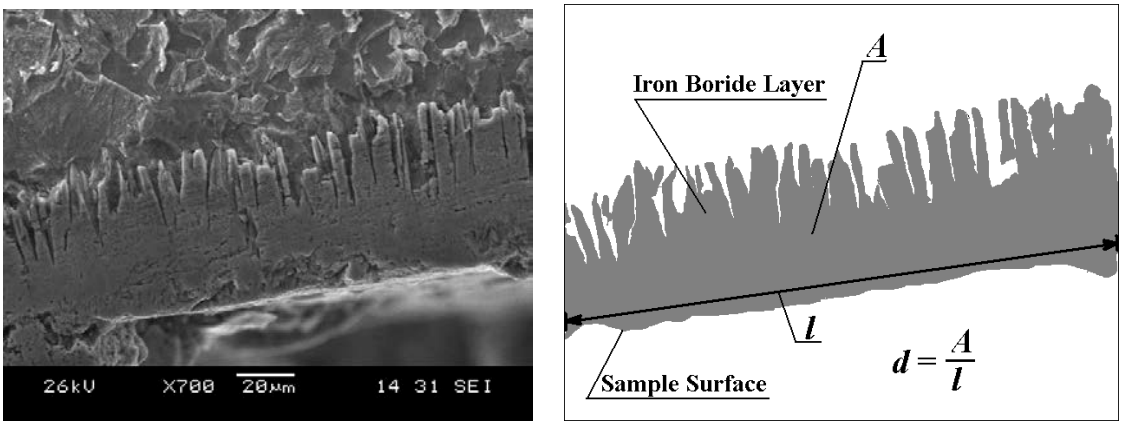

Figure 1 Schematic diagram illustrating the procedure for the estimation of boride layer thickness.

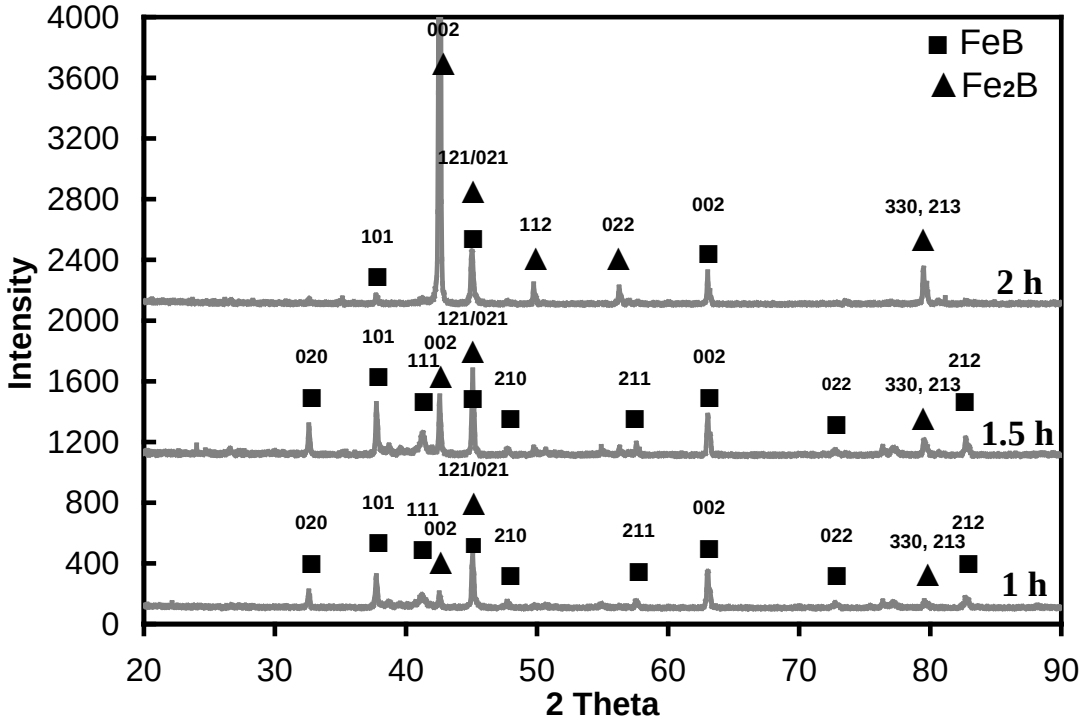

(a) Boriding for 60, 90 and 120 minutes

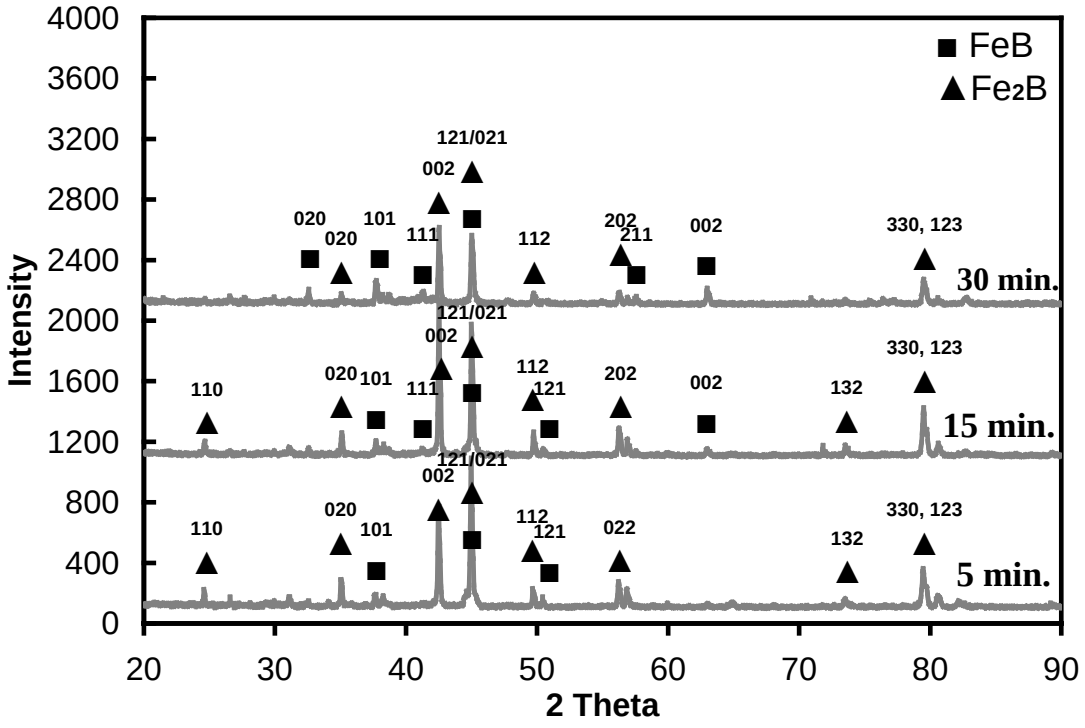

(b) Boriding for 5, 15 and 30 minutes

Figure 2. XRD results for mild still samples borided at 850˚C for different durations

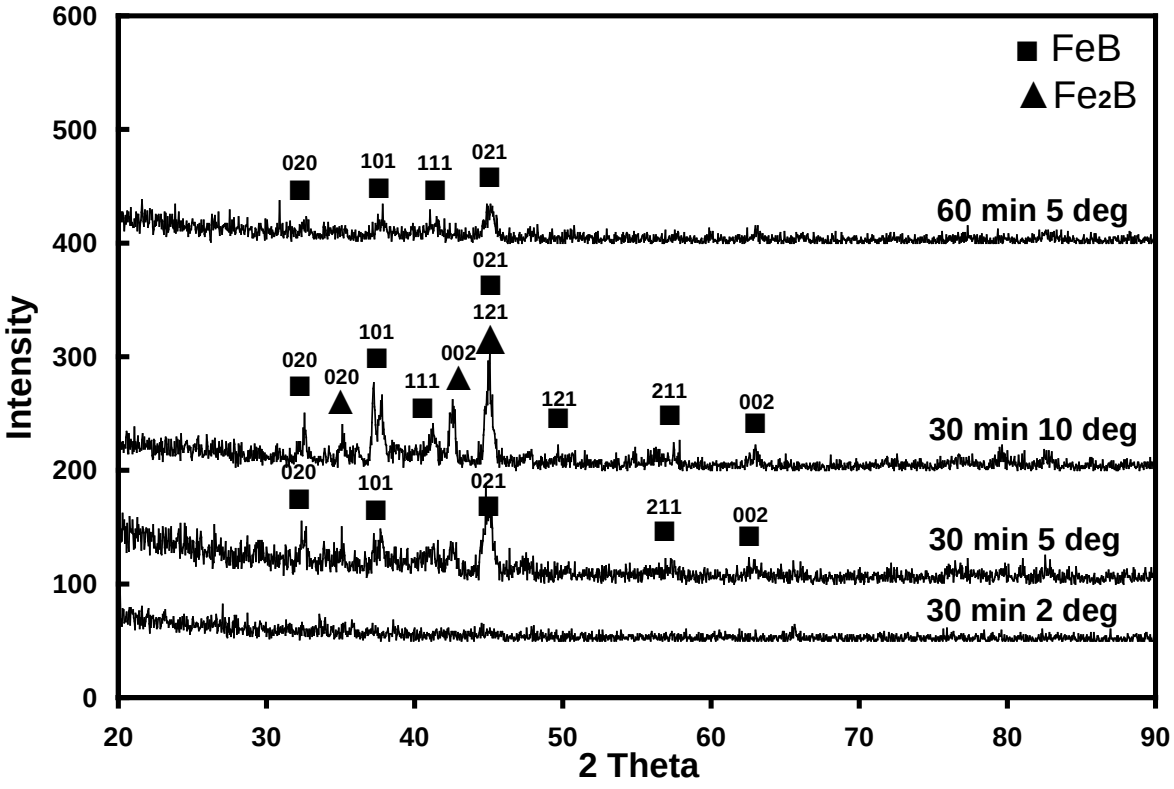

Figure 3 Phase composition analyzed by grazing XRD (Grazing angle: 2, 5 and 10 degrees for sample borided for 30 min., and 5 degree for sample borided for 60 min.)

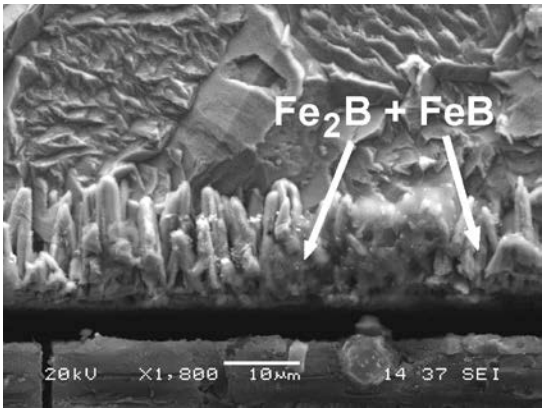

(a) 5 minutes, 1800×

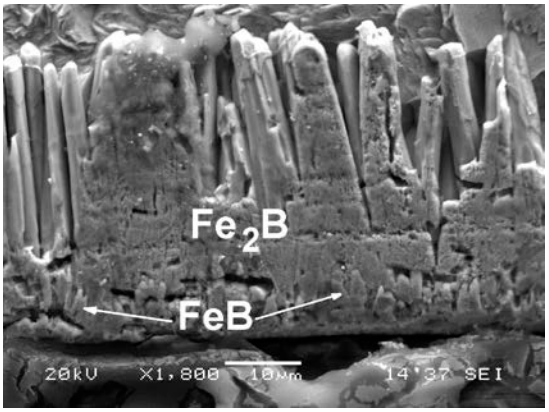

(b) 30 minutes, 1800×

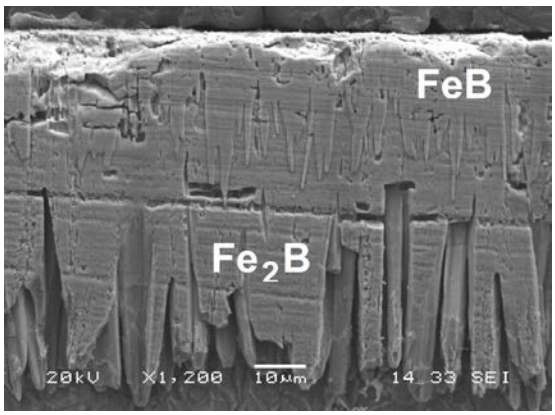

(c) 60 minutes, 1200×

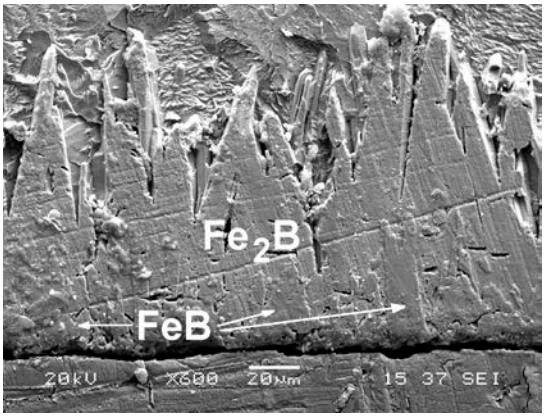

(d) 90 minutes, 600×

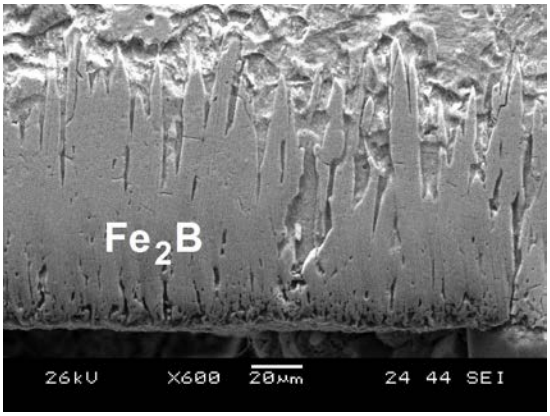

(e) 120 minutes, 600×

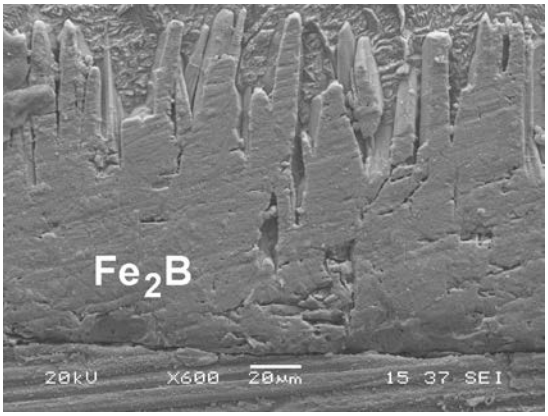

(f) 240 minutes, 600×

Figure 4. SEM pictures for mild steel borided at 850˚C for different durations

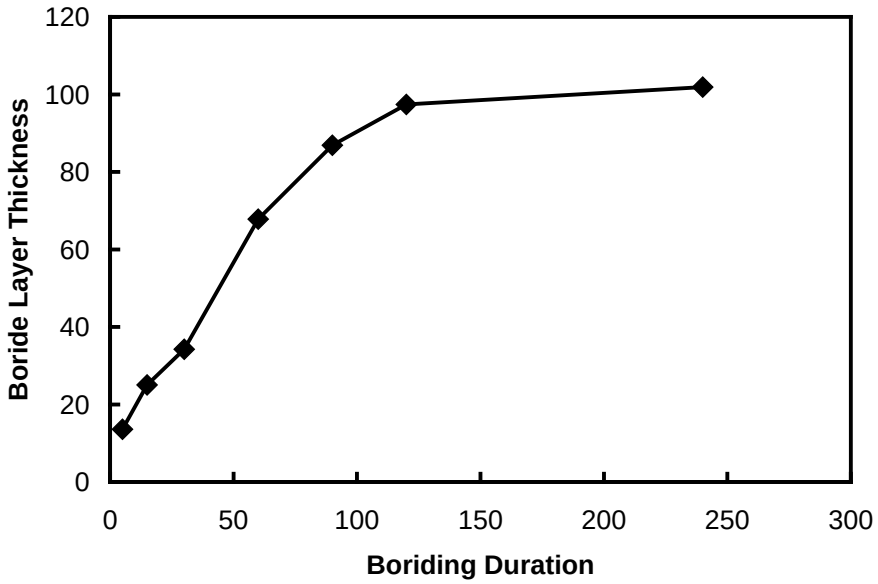

Figure 5. Boride layer thickness vs. boriding duration

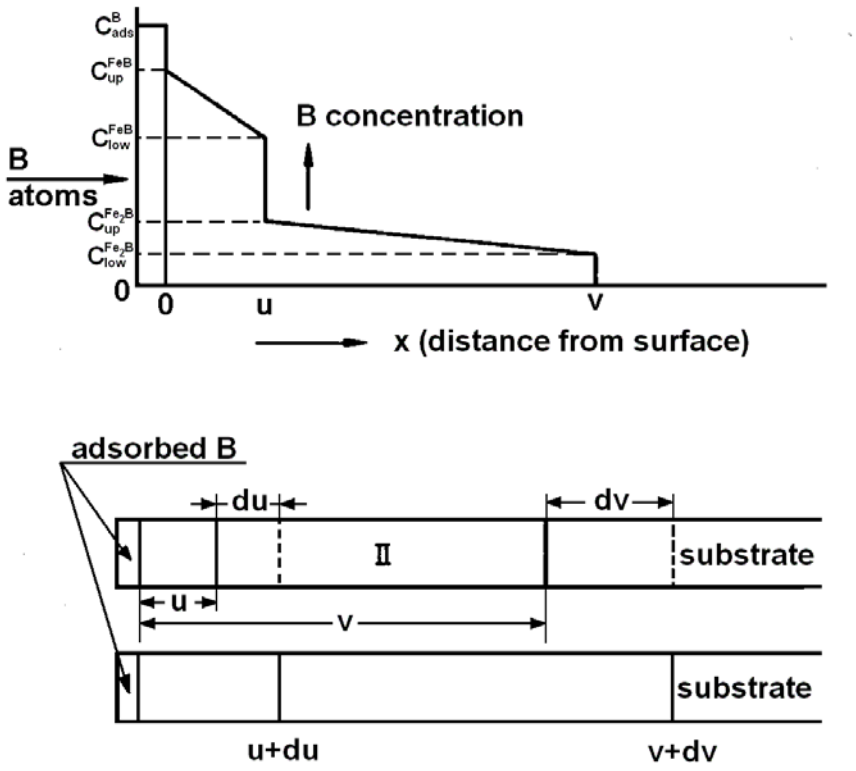

Figure 6. Boron concentration profile assumed in the numerical simulation

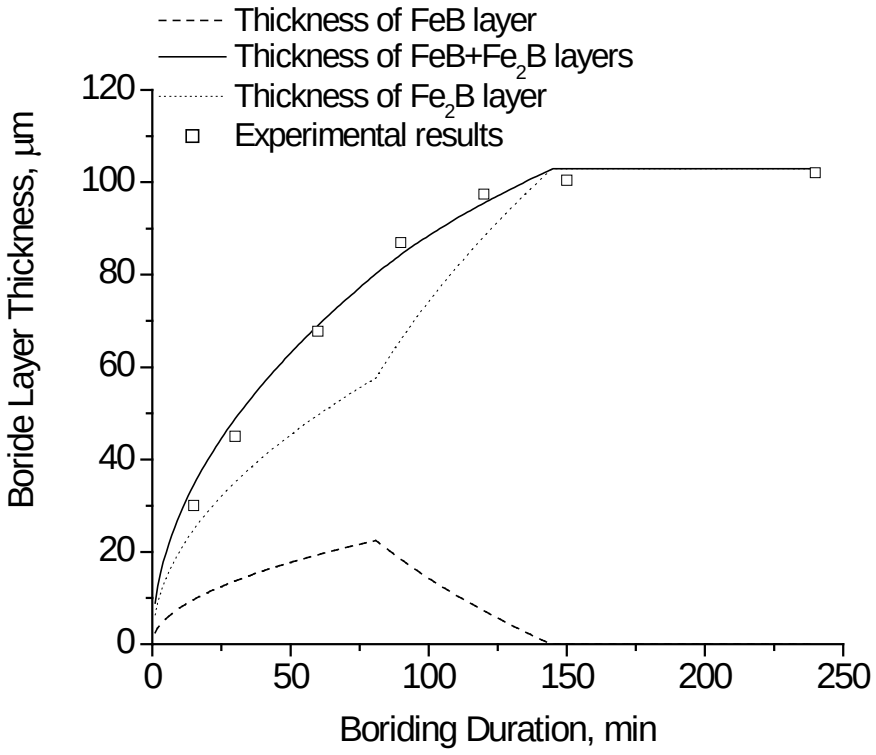

Figure 7. Simulated boride-layer growth vs. boriding duration.